This article was downloaded by:[Battelle for the USDOE]
On: 3 March 2008
Access Details: [subscription number 777257314]
Publisher: Informa Healthcare
Informa Ltd Registered in England and Wales Registered Number: 1072954
Registered office: Mortimer House, 37-41 Mortimer Street, London W1T 3JH, UK

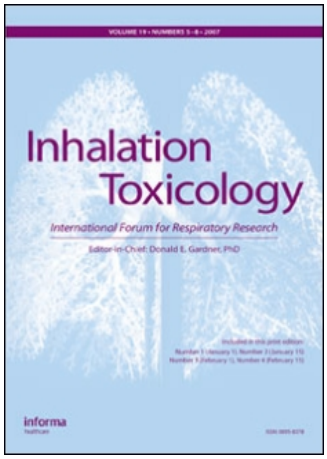

Inhalation Toxicology
International Forum for Respiratory Research
Publication details, including instructions for authors and subscription information:
http://www.informaworld.com/smpp/title~content=t713657711

A PBPK Model for Evaluating the Impact of Aldehyde Dehydrogenase Polymorphisms on Comparative Rat and Human Nasal Tissue Acetaldehyde Dosimetry

Justin G. Teeguarden [a]; Matthew S. Bogdanffy [b]; Tammie R. Covington [c]; Cecilia Tan [d]; Annie M. Jarabek [e]
[a] Biological Monitoring and Modeling, Pacific Northwest National Laboratory, Richland, Washington, USA
[b] Boehringer Ingelheim Pharmaceuticals, Ridgefield, Connecticut, USA
[c] Human Effectiveness Directorate, Air Force Research Laboratory, Wright Patterson AFB, Dayton, Ohio, USA
[d] The Hamner Institutes for Health Sciences, Research Triangle Park, North Carolina, USA
[e] U.S. EPA, Office of Research and Development, National Health Effects Research Laboratory, Experimental Toxicology Division, Pharmacokinetics Branch, Research Triangle Park, North Carolina, USA

Online Publication Date: 01 February 2008
To cite this Article: Teeguarden, Justin G., Bogdanffy, Matthew S., Covington, Tammie R., Tan, Cecilia and Jarabek, Annie M. (2008) 'A PBPK Model for Evaluating the Impact of Aldehyde Dehydrogenase Polymorphisms on Comparative Rat and Human Nasal Tissue Acetaldehyde Dosimetry', Inhalation Toxicology, 20:4, 375 - 390
To link to this article: DOI: 10.1080/08958370801903750
URL: http://dx.doi.org/10.1080/08958370801903750

PLEASE SCROLL DOWN FOR ARTICLE

Full terms and conditions of use: http://www.informaworld.com/terms-and-conditions-of-access.pdf

This article maybe used for research, teaching and private study purposes. Any substantial or systematic reproduction, re-distribution, re-selling, loan or sub-licensing, systematic supply or distribution in any form to anyone is expressly forbidden.

The publisher does not give any warranty express or implied or make any representation that the contents will be complete or accurate or up to date. The accuracy of any instructions, formulae and drug doses should be independently verified with primary sources. The publisher shall not be liable for any loss, actions, claims, proceedings, demand or costs or damages whatsoever or howsoever caused arising directly or indirectly in connection with or arising out of the use of this material.

Downloaded By: [Battelle for the USDOE] At: 15:18 3 March 2008

Inhalation Toxicology, 20:375–390, 2008
Copyright © Informa Healthcare USA, Inc.
ISSN: 0895-8378 print / 1091-7691 online
DOI: 10.1080/08958370801903750

informa
healthcare

A PBPK Model for Evaluating the Impact of Aldehyde Dehydrogenase Polymorphisms on Comparative Rat and Human Nasal Tissue Acetaldehyde Dosimetry

Justin G. Teeguarden
Biological Monitoring and Modeling, Pacific Northwest National Laboratory, Richland, Washington, USA

Matthew S. Bogdanffy
Boehringer Ingelheim Pharmaceuticals, Ridgefield, Connecticut, USA

Tammie R. Covington
Human Effectiveness Directorate, Air Force Research Laboratory, Wright Patterson AFB, Dayton, Ohio, USA

Cecilia Tan
The Hamner Institutes for Health Sciences, Research Triangle Park, North Carolina, USA

Annie M. Jarabek
U.S. EPA, Office of Research and Development, National Health Effects Research Laboratory, Experimental Toxicology Division, Pharmacokinetics Branch, Research Triangle Park, North Carolina, USA

Acetaldehyde is an important intermediate in the chemical synthesis and normal oxidative metabolism of several industrially important compounds, including ethanol, ethyl acetate, and vinyl acetate. Chronic inhalation of acetaldehyde leads to degeneration of the olfactory and respiratory epithelium in rats at concentrations >50 ppm (90 day exposure) and respiratory and olfactory nasal tumors at concentrations ≥750 ppm, the lowest concentration tested in the 2-yr chronic bioassay. Differences in the anatomy and biochemistry of the rodent and human nose, including polymorphisms in human high-affinity acetaldehyde dehydrogenase (ALDH2), are important considerations for interspecies extrapolations in the risk assessment of acetaldehyde. A physiologically based pharmacokinetic model of rat and human nasal tissues was constructed for acetaldehyde to support a dosimetry-based risk assessment for acetaldehyde (Dorman et al., 2008). The rodent model was developed using published metabolic constants and calibrated using upper-respiratory-tract acetaldehyde extraction data. The human nasal model incorporates previously published tissue volumes, blood flows, and acetaldehyde metabolic constants. ALDH2 polymorphisms were represented in the human model as reduced rates of acetaldehyde metabolism. Steady-state dorsal olfactory epithelial tissue acetaldehyde concentrations in the rat were predicted to be 409, 6287, and 12,634 μM at noncytotoxic (50 ppm), and cytotoxic/tumorigenic exposure concentrations (750 and 1500 ppm), respectively. The human equivalent concentration (HEC) of the rat no-observed-adverse-effect level (NOAEL)

Received 10 June 2007; accepted 29 October 2007.
The authors acknowledge the Vinyl Acetate Council for funding the development of the acetaldehyde model. The authors also acknowledge Dr. Jerry Campbell of The Hamner Institutes for his technical assistance with the modeling.
This document has been subjected to review by the National Health and Environmental Effects Research Laboratory and approved for publication. Approval does not signify that the contents reflect the views of the agency, nor does mention of trade names or commercial products constitute endorsement or recommendation for use. The U.S. government has the right to retain a nonexclusive, royalty-free copyright covering this article.
Address correspondence to Justin G. Teeguarden, Biological Monitoring and Modeling, Pacific Northwest National Laboratory, 902 Battelle Boulevard, P7-56, Richland, WA 99352, USA. E-mail: justin.teeguarden@pnl.gov

Downloaded By: [Battelle for the USDOE] At: 15:18 3 March 2008

of 50 ppm, based on steady-state acetaldehyde concentrations from continual exposures, was 67 ppm. Respiratory and olfactory epithelial tissue acetaldehyde and H^+ (pH) concentrations were largely linear functions of exposure in both species. The impact of presumed ALDH2 polymorphisms on human olfactory tissue concentrations was negligible; the high-affinity, low-capacity ALDH2 does not contribute significantly to acetaldehyde metabolism in the nasal tissues. The human equivalent acetaldehyde concentration for homozygous low activity was 66 ppm, 1.5% lower than for the homozygous full activity phenotype. The rat and human acetaldehyde PBPK models developed here can also be used as a bridge between acetaldehyde dose-response and mode-of-action data as well as between similar databases for other acetaldehyde-producing nasal toxicants.

Acetaldehyde is an important industrial chemical, common air pollutant, and endogenous by-product of normal metabolism (Jones, 1995a). Acetaldehyde occurs naturally in many foods (Feron et al., 1991) and is exhaled at parts per billion levels by humans in the absence of alcohol intake (Jones, 1995a). Acetaldehyde is a relatively weak clastogen that induces sister-chromatid exchanges and reacts with DNA to form DNA–protein and DNA–DNA cross-links (Dellarco, 1988). Chronic inhalation exposure to acetaldehyde causes increased incidence of nasal tumors in rats (Feron et al., 1982; Woutersen et al., 1984, 1986; Woutersen & Feron, 1987). Male and female Wistar rats exposed by inhalation to 0, 750, 1500, or 3000 ppm acetaldehyde for 6 h/day, 5 days/wk for up to 28 mo (Woutersen et al., 1984, 1986) developed olfactory adenocarcinomas at all exposure levels. Respiratory squamous-cell carcinomas were found in male rats at the mid and high concentrations and in female rats only at the high concentration. The incidence of carcinomas was greatest in the olfactory epithelium. Both types of tumors were also found in rats exposed to the same concentrations of acetaldehyde for 52 wk and followed for 26 wk or 52 wk of recovery (Woutersen & Feron, 1987). Epithelial degeneration, a probable precursor to tumor development, is also observed after chronic exposure to acetaldehyde, particularly in the olfactory epithelium, which is more sensitive to cellular toxicity than is the respiratory epithelium (Appelman et al., 1982, 1986).

Acetaldehyde is metabolized to acetate by aldehyde dehydrogenase (ALDH) (Jakoby et al., 1982), a detoxifying pathway in most tissues, including the nasal tissues of rodents and humans. Protons (H^+) are a by-product of acetaldehyde metabolism with the potential, under conditions of high exposure where cellular buffering systems and proton pumps may be overwhelmed, to acidify cells (Bogdanffy et al., 2001) and cause cytotoxicity. In rodent nasal olfactory and respiratory tissues, low-affinity (cytosolic, ALDH1) and high-affinity (mitochondrial, ALDH2) pathways for acetaldehyde metabolism have been described (Bogdanffy et al., 1998; Casanova-Schmitz et al., 1984; Morris, 1997). These same low- and high-affinity pathways (Yoshida, 1992) are present in human tissues (Franklin & Johnson, 1994; Ginsberg et al., 2002; Oyama et al., 2005; Stewart et al., 1996). ALDH2 protein or mRNA has been measured in human liver, kidney, muscle, heart, esophagus, spleen, thymus, prostate, testis, ovary, peripheral blood lymphocytes, and intestinal mucosa (Franklin & Johnson, 1994; Oyama et al., 2005; Stewart et al., 1996) and in fetal brain and lung. The distribution of ALDH2 expression in humans is similar to that in rodents for tissues that have been studied. ALDH2 is expressed in multiple mouse tissues including nasal tissues, liver, lung, testis, esophagus, stomach, colon, and pancreas (Morris, 1997; Oyama et al., 2005). In the rat, ALDH2 expression is similarly distributed—kidney, liver, lung, heart, spleen, and nasal tissues (Morris, 1997; Yoon et al., 2006). Hamster and guinea pig nasal tissues also show evidence of an ALDH2 pathway (Morris, 1997). Human nasal tissue has not been assayed for ALDH2, but given the wide tissue distribution of ALDH2 in humans and in mice and rats, and the evidence of a high-affinity pathway in the nasal tissue of multiple rodent species, it is plausible that ALDH2 is expressed in human nasal tissues.

Two key variants of ALDH2 have been identified in humans and rodents: ALDH2*1, an active form of the enzyme that is dominant in most populations studied, and ALDH2*2, an inactive form of the enzyme that is relatively common only in Asians. Three genotypes and their corresponding phenotypes are expected: a fully active homozygote (ALDH2*1/1), an intermediate activity heterozygote (ALDH2*1/2), and a zero-activity homozygote (ALDH2*2/2).

Nasal tissue concentrations of two dose metrics important for risk assessment purposes, namely, acetaldehyde and H^+, are expected to be impacted by the activity of ALDH. ALDH2 was recently hypothesized to be particularly important to tissue levels of acetaldehyde at low exposure concentrations (Ginsberg et al., 2002) of acetaldehyde and compounds producing acetaldehyde in the course of normal metabolism. A rich literature describes the molecular epidemiology of alcohol metabolism-related diseases and deficiencies in alcohol and aldehyde metabolism, but this work has not been extended to evaluate potential impacts on the toxicity of inhaled acetaldehyde or acetaldehyde producing compounds.

A mode of action (MOA)-based cancer risk assessment for vinyl acetate, an acetaldehyde- and H^+-producing chemical, has been developed based on a proposed mode of action for pathogenesis of nasal tumors that identifies the key event as intracellular acidification of nasal tissues leading to cytotoxicity and compensatory cell proliferation. In rodents exposed by inhalation to high concentrations of vinyl acetate, and therefore nasal tissue coexposed to acetaldehyde and H^+, or in rodents exposed to acetaldehyde directly, nasal tumors are observed at exposures causing cytotoxicity (e.g., epithelial degeneration), but in the case of vinyl acetate, not at lower concentrations (50 ppm) (Appelman et al., 1982, 1986; Bogdanffy et al., 1999b; Bogdanffy & Taylor, 1993; Woutersen et al., 1984, 1986). Vinyl acetate and acetaldehyde have in common key elements of a mode of action for nasal tissue carcinogenicity and two potential toxicants: acetaldehyde and H^+. The relative amounts of these two chemicals in nasal tissues are therefore expected to be correlated with the tumor dose-response for vinyl acetate and acetaldehyde. Both

Downloaded By: [Battelle for the USDOE] At: 15:18 3 March 2008

vinyl acetate and acetaldehyde are undergoing Integrated Risk Information System (IRIS) review. A parallel risk assessment for acetaldehyde, the subject of the companion article to this article, was developed by Dorman et al. (2008). A physiologically based pharmacokinetic (PBPK) model of the upper respiratory tract has been developed to conduct interspecies extrapolation of nasal tissue dosimetry for vinyl acetate (Plowchalk et al., 1997), but no such model exists for acetaldehyde.

The objective of this work was to develop an acetaldehyde upper-respiratory-tract PBPK model of the same general structure as the vinyl acetate PBPK model to both evaluate interspecies differences in tissue acetaldehyde and H^+ dosimetry and explore the potential impact of ALDH2 polymorphisms on human nasal tissue dosimetry. The relationships between acetaldehyde exposure and dorsal olfactory tissue acetaldehyde concentrations in rats and humans were used by Dorman et al. to support a chemical-specific dosimetric adjustment from rodents to humans for risk assessment (Dorman et al. 2008).

METHODS

Overview of Approach

The development and application of the acetaldehyde upper-respiratory-tract model followed several distinct steps (Figure 1) described in further detail in the following sections. The acetaldehyde submodel of the published vinyl acetate model (Plowchalk et al., 1997) was revised for direct inhalation of acetaldehyde, retaining all physiological, biochemical, and physicochemical parameters as they appeared in the published vinyl acetate model. The ALDH2 Vmax values for the rat respiratory and olfactory tissues were then calibrated against acetaldehyde upper-respiratory-tract extraction data (Plowchalk et al., 1997). Once the parameterization was complete, a pH submodel identical to the used by Plowchalk et al. (1997) was added to simulate pH changes in acetaldehyde metabolizing tissues and rat nasal tissue dosimetry was estimated across a wide range of inhaled acetaldehyde concentrations. The human acetaldehyde model was then exercised to determine the human equivalent concentration of acetaldehyde. Finally, the human model was revised to account for plausible reductions in high-affinity nasal tissue acetaldehyde metabolism due to observed genetic ALDH2 polymorphisms, and the effect of presumed polymorphisms on nasal tissue dosimetry and the human equivalent concentration (HEC) were determined.

Model Structure

The acetaldehyde upper airway PBPK model is structurally the same as the inhalation-route vinyl acetate model (Bogdanffy et al., 1999a). The airway model for acetaldehyde consists of

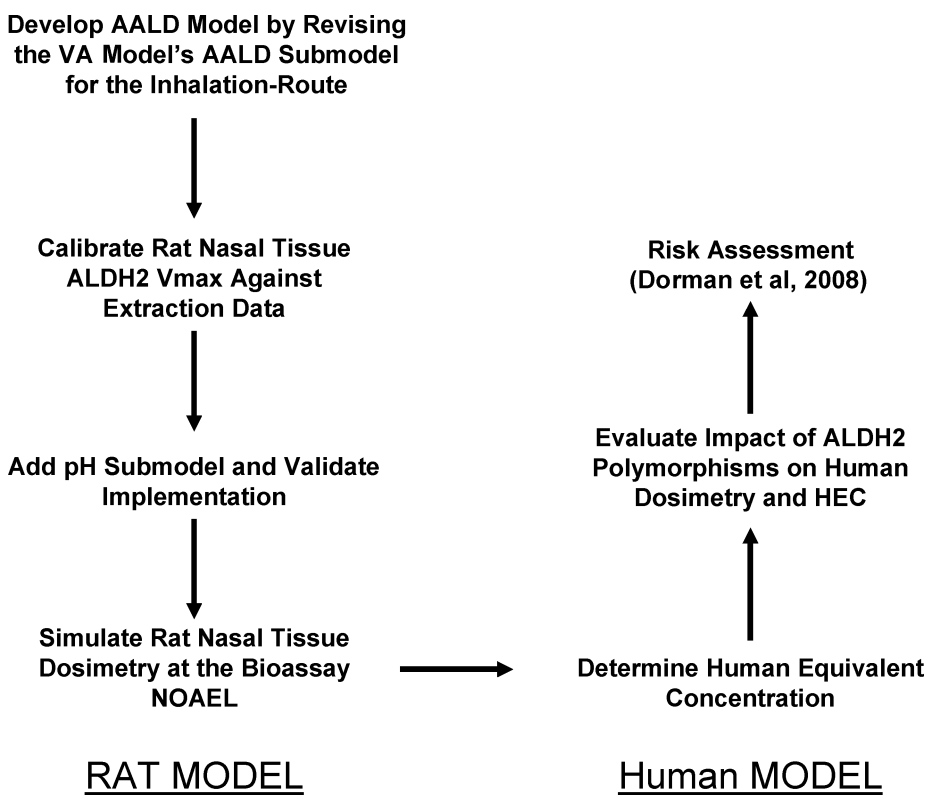

FIG. 1. Diagram describing the steps taken in the development and application of the acetaldehyde (AALD) upper-respiratory-tract PBPK model.

Downloaded By: [Battelle for the USDOE] At: 15:18 3 March 2008

the nasal cavity, nasopharynx, and larynx. The primary focus of this model is the nasal cavity, which forms the portal of entry for inhaled compounds and is the target site for acetaldehyde-induced lesions. The nasal cavity has a complex anatomy with a variety of tissue types. Inspired air follows distinct pathways within the nasal cavity, resulting in asymmetric ventilation of the various regions in the nasal cavity. Computational fluid dynamic models identify two distinct flow pathways in the nasal cavity in both rats and humans: a dorsal/medial pathway and a lateral/ventral pathway (Kimbell et al., 1997; Subramaniam et al., 1998). Along the dorsal airstream in the rat is an anterior patch of respiratory epithelium, and posterior to this is the entire ethmoid turbinate region lined by olfactory epithelium. The ventral side consists of the remaining portions of the rat nasal passage lined with respiratory epithelium. The compartmentalization of the nasal cavity in the model follows this inherent division in tissue type and location. The rat nasal cavity model has five major compartments, one representing the dorsal respiratory tissue, two representing the dorsal olfactory tissue, and two representing the ventral respiratory tissue (Figure 2). The human model structure reduces the two dorsal olfactory tissue compartments to one. The size of the human dorsal olfactory tissue is small enough that a significant anterior–posterior concentration gradient is not expected, eliminating the need to represent it as two tissues. Because the contribution of arterial blood acetaldehyde from pulmonary uptake to nasal tissue concentrations was vanishingly small (confirmed by simulation), compartments posterior to the nasopharyx representing pulmonary uptake, distribution, and metabolic elimination are not considered. The compartmental structure of the nasal compartment and the associated anatomical parameter values are the same as the published vinyl acetate model (Plowchalk et al., 1997).

The respiratory-tract tissues receive acetaldehyde from inhaled air and blood flow. To represent the various processes that transport acetaldehyde and its metabolites to the epithelial cell layer, the five nasal cavity compartments were divided into a three-layered substructure, as proposed previously (Morris et al., 1993). This three-layer structure consists of a lumen, an epithelial cell layer, and a submucosal tissue layer (Figure 2). The lumen is ventilated by the inhaled air, and the submucosal tissue layer is perfused by blood that clears acetaldehyde and its metabolites from the tissue. The epithelial cell layer, which expresses enzymes for metabolism of acetaldehyde and its downstream metabolite acetic acid, forms the target site for toxicity. The mucous layer specified in the vinyl acetate model (Plowchalk et al., 1997) because it was a site of vinyl acetate metabolism is not an explicit compartment in this model; the mucous layer was lumped with the epithelial cell layer because the mucous layer is not a site of acetaldehyde metabolism.

Acetaldehyde is metabolized to acetic acid by ALDH (Jakoby et al., 1982), which is subsequently cleared by acetyl coenzyme A (CoA) synthetase (ACS) (Knowles et al., 1974). Metabolism of acetaldehyde by ALDH in the nasal cavity is modeled as two saturable processes comprising one high-capacity, low-affinity (ALDH1) and one low-capacity, high-affinity pathway (ALDH2), both following Michaelis–Menten kinetics. Acetic acid is metabolized by ACS (Knowles et al., 1974) and is cleared from the tissue according to Michaelis–Menten kinetics. Acetaldehyde metabolism is assumed to be distributed in the nasal compartments according to previously reported histochemical data (Bogdanffy et al., 1986) and is consistent with the distribution used in the published vinyl acetate model (Plowchalk et al., 1997) (Table 1). The model was coded to account for the production of two protons for every molecule of acetaldehyde metabolized according to Plowchalk (Plowchalk et al., 1997).

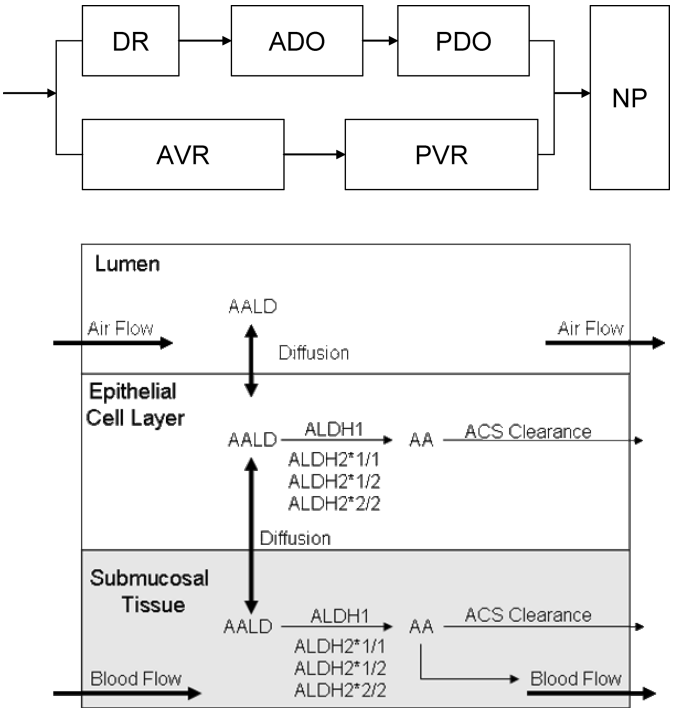

FIG. 2. Top panel: Compartmental structure of the hybrid CFD/PBPK model of the upper airways. A, anterior; P, posterior; D, dorsal; V, ventral; O, Olfactory; R, respiratory; NP, nasal pharyngeal. Arrows indicate the air flow pattern. Bottom panel: Schematic of the three-layered structure of each tissue compartment showing the various metabolic and transport pathways for acetaldehyde. AA, acetic acid; ALDH1, low-affinity acetaldehyde dehydrogenase; ALDH2*1/1, ALDH2*1/2, ALDH2*2/2, full, intermediate, and low-activity high-affinity acetaldehyde dehydrogenase; ACS, acetyl CoA synthetase.

Unidirectional airflow is assumed in the nasal cavity. The analytical expressions that describe the transport of an inhaled chemical across the lumen and tissue subcompartments in the nasal cavity have been described elsewhere in detail (Andersen et al., 1999; Bogdanffy et al., 1999b) and are presented in brief form here in Appendix A.

A pH submodel was introduced into the respiratory epithelium and olfactory submucosa, the two tissue subcompartments

Downloaded By: [Battelle for the USDOE] At: 15:18 3 March 2008

TABLE 1
Model parameters

Parameter	Rat	Human	Reference
Flows parameters			
Cardiac output (CO) (ml/min)	110	7500	(Brown et al., 1997)
Nasal cavity blood flow (% CO)	0.1	0.25	(Holmberg et al., 1989; Paulsson et al., 1985; Stott et al., 1986)
Minute ventilation (MV) (ml/min)	200–260	13,890	Experimental Conditions
Dorsal nasal cavity air flow (% MV)	0.15	0.075	(Kimbell et al., 1997)
Ventral nasal cavity air flow (% MV)	0.85	0.925	(Kimbell et al., 1997)
Tissue surface areas (cm^2)			
Dorsal respiratory	0.2	10.1	(Bogdanffy et al., 1999b)
Anterior dorsal olfactory	0.42	13.2	(Bogdanffy et al., 1999b)
Posterior dorsal olfactory	6.33	—	(Bogdanffy et al., 1999b)
Anterior ventral respiratory	1.8	42.1	(Bogdanffy et al., 1999b)
Posterior ventral respiratory	4.5	72.3	(Bogdanffy et al., 1999b)
Mucus thickness (cm)[g]	0.001	0.001	(Plowchalk et al., 1997)
Epithelial tissue thickness (cm)			
Dorsal respiratory	0.005	0.005[a]	(Bogdanffy et al., 1999b)
Anterior dorsal olfactory	0.005[a]	—	(Bogdanffy et al., 1999b)
Posterior dorsal olfactory	0.005[a]	0.004[a]	(Bogdanffy et al., 1999b)
Anterior ventral respiratory	0.005	0.005[b]	(Bogdanffy et al., 1999b)
Posterior ventral respiratory	0.005	0.005[b]	(Bogdanffy et al., 1999b)
Submucosa thickness (cm)			
Dorsal respiratory	0.002	0.002[b]	(Plowchalk et al., 1997)
Anterior dorsal olfactory	0.002	—	(Plowchalk et al., 1997)
Posterior dorsal olfactory	0.002	0.002[b]	(Plowchalk et al., 1997)
Anterior ventral respiratory	0.002	0.002[b]	(Plowchalk et al., 1997)
Posterior ventral respiratory	0.002	0.002[b]	(Plowchalk et al., 1997)
Lumen volumes (cm^3)			
Dorsal respiratory	0.004	0.74	(Bogdanffy et al., 1999b)
Anterior dorsal olfactory	0.012	0.56	(Bogdanffy et al., 1999b)
Posterior dorsal olfactory	0.054	—	(Bogdanffy et al., 1999b)
Anterior ventral respiratory	0.09	3.5	(Bogdanffy et al., 1999b)
Posterior ventral respiratory	0.09	5.16	(Bogdanffy et al., 1999b)
Air-phase mass transfer coefficients (cm/min)			
Dorsal respiratory	19,980	197	(Frederick et al., 1998)
Anterior dorsal olfactory	8040	1368	(Frederick et al., 1998)
Posterior dorsal olfactory	26,520	—	(Frederick et al., 1998)
Anterior ventral respiratory	34,680	158	(Frederick et al., 1998)
Posterior ventral respiratory	184,980	194	(Frederick et al., 1998)
Partition coefficient			
Acetaldehyde blood/air	224	190	(Jones, 1995b; Plowchalk et al., 1997)
Acetaldehyde tissue/blood	1	1	(Plowchalk et al., 1997)
Acetone blood/air	80,000	80,000	(Plowchalk et al., 1997)
Acetone tissue/blood	1	1	(Plowchalk et al., 1997)
Metabolism—acetaldehyde Vmax (nmol/min/ml)			
Respiratory epithelium (low affinity, high Km)	53,307	53,596	(Bogdanffy et al., 1998)
Olfactory epithelium (low affinity, high Km)	0.0[a]	0.0[a]	(Bogdanffy et al., 1998)

(Continued on next page)

Downloaded By: [Battelle for the USDOE] At: 15:18 3 March 2008

TABLE 1
Model parameters (*Continued*)

Parameter	Rat	Human	Reference
Olfactory submucosa (low affinity, high Km)	16,588	16,549	(Bogdanffy et al., 1998)
Respiratory epithelium (high affinity, low Km)	600[c]	600[d]	Optimized to URT extraction data
Olfactory epithelium (high affinity, low Km)	0.0	0.0	(Plowchalk et al., 1997)
Olfactory submucosa (high affinity, low Km)	600[c]	600[d]	Optimized to URT extraction data
Km (nmol/ml)			
Respiratory/olfactory (high Km)	18,100	25,000	(Bogdanffy et al., 1998)
Respiratory/olfactory (low Km)	30	30[e]	(Morris, 1997)
Metabolism—acetate Vmax (nmoles/min/ml)			
Olfactory epithelium	2550[f]	2550[e]	(Knowles et al., 1974)
Respiratory epithelium	2550[f]	2550[e]	(Knowles et al., 1974)
Km (nmol/ml)	300[f]	300[5]	(Knowles et al., 1974)
Diffusivity constants (cm^2/min)	0.0002	0.0002	CRC Physical and Chemical Handbook

[a]The value listed does not appear in the listed citation, but we have confirmed through the author (and direct inspection) that the value was used in the modeling described in the citation. The value differs from the sustentacular cell apical cytoplasm depth listed in Table 2 of the 1998 manuscript (Bogdanffy et al., 1998). The sustentacular cell apical cytoplasm depth represents only a portion of the total cell depth and underrepresents the total tissue depth.

[b]The value listed does not appear in the listed citation, but we have confirmed through the author (and direct inspection) that the value was used in the modeling described in the citation. The experimentally measured tissue depth is 0.0045 cm (Bogdanffy et al., 1998). Bogdanffy (1999b) used 5 equal tissue stacks of 0.001 cm to represent the tissue (0.005 cm total depth), which we chose to be consistent with.

[c]Optimized to rat URT extraction dataof Morris (1997).

[d]Scaled from rat value using the ratio of activities of the high-affinity Km ALDH2 in human/rat reported by Bogdanffy (Bogdanffy et al., 1998), as converted to a per ml tissue basis and reported in Table 1. The value was 1.0 for epithelial tissues and 1.0 for the submucosa.

[e]Assumed equivalent to the rat value.

[f]Assumed equal to hepatic value.

[g]A mucus thickness is specified in Table 2, but this compartment is not explicitly represented in the model. The mucous layer is part of a lumped compartment composed of the epithelium and the mucous layer.

producing protons through acetaldehyde metabolism, given the available information on tissue localization of ALDH. The pH submodel used here, including the associated parameters, is identical to those used by Bogdanffy (Bogdanffy et al., 1999b) and Plowchalk (Plowchalk et al., 1997). A quadratic form of the submodel was used:

$$H^+_{Buffered} = \{KA + H^+_{Total} + A_{Total} - SQRT[(H^+_{Total} + KA)^2 + A_{Total} * (A_{Total} + 2 * KA - 2 * H^+_{Total})]\}/2$$

$$H^+_{Free} = H^+_{Total} - H^+_{Buffered}$$

where $H^+_{Buffered}$ is the concentration of protons bound to buffering compounds, H^+_{Total} is the total proton concentration, H^+_{Free} is the free concentration of protons, KA is the disassociation constant (antilog of the pK_a) of the cellular buffering material, A_{Total} is the total concentration of buffering materials, and pH is computed as log (H^+_{Free}). All concentrations have units of molar concentration. The model parameters are provided in Table 2. The mathematical formulation of the pH model was verified by comparing the pH resulting from exposures to vinyl acetate (using the vinyl acetate model) and acetaldehyde that result in the same steady-state proton production rate within the nasal tissues (personal communication, Paul Hinderliter, PNNL). The predictions of cellular pH have not been verified experimentally. The pH submodel is included here because it nonetheless captures and describes inherent nonlinearities in pH as a function

TABLE 2
pH Submodel parameters

Parameter	Value[a]
Initial pH	7.4
Composite intracellular buffer concentration	70 m*M*
Composite intracellular buffer pK_a	6.8
Na^+/H^+ Antiport Vmax	63.7 mmol/L/min[JGT2]
Na^+/H^+ Antiport K_H	2.9×10^{-4} mmol/L
Na^+/H^+ Antiport Hill coefficient	1.97

[a]As reported (Plowchalk et al., 1997). The pH submodel used here is identical to the one used by Plowchalk et al. (1997) (see Methods, pH submodel).

Downloaded By: [Battelle for the USDOE] At: 15:18 3 March 2008

of acetaldehyde exposure, which can be explored experimentally and serve to revise the pH submodel as needed at a later time.

Model Parameterization

Flow parameters, mass transfer coefficients, partition coefficients, lumen volumes, tissue surface areas, and thicknesses were used as described by others in similar models of the upper respiratory tract. These parameters are summarized in Table 1.

The initial Michealis–Menten maximum velocity (Vmax) for ALDH1 was estimated by distributing the whole-nose activity (rat and human, mg/h), measured separately for olfactory and respiratory tissue (Bogdanffy et al., 1998) according to volumes of these tissues used in the model (Table 1). The calculation of tissue-specific ALDH1 activities is presented in Appendix B. This approach assured that the total ALDH1 activity reported and used by Bogdanffy (Bogdanffy et al., 1998) in the vinyl acetate model would be maintained in the acetaldehyde model. The rat Vmax for ALDH2 was estimated by fitting to data on the extraction of acetaldehyde from the isolated upper respiratory tract (URT) of rats exposed unidirectionally at various flow rates and acetaldehyde concentrations as reported by (Morris, 1997) (see Results).

The Km for the ALDH1 pathway was used directly as reported by Bogdanffy (1998). The Km for the ALDH2 pathway was used as reported by Morris (1997). The ALDH2 polymorphisms were assumed to have no significant impact on the ALDH2 Km. This is plausible because the activities of the polymorphs are described as high-affinity enzymes, indicating that the Km for this form of ALDH has not changed enough to change its designation from high to low affinity.

In the absence of a tested approach for allometrically scaling the rat nasal activity for use in the human model, it was assumed that the ratio of Vmax values (nmol/min/ml tissue) for ALDH1 in rats and humans describes the relationship between the activities of ALDH2 in these two species. For both respiratory and olfactory tissues, this ratio was one. Scaling the rat high-affinity Vmax values to estimate the human values using this relationship results in equivalent ALDH2 activities in these species on a per milliliter tissue basis. Alternative approaches, such as body weight scaling, were also considered for scaling rat Vmax values for use in the human model, but were not used because adopting such an approach results in much higher Vmax values in humans, which is unexpected. For instance, the size of the olfactory tissues in the human is smaller and enzyme activities lower in some cases than the rat. Allometric scaling is particularly relevant for scaling activities in organs whose function is conserved across species. In general, we felt that this did not hold as well for the human nose as it would for other organs such as the liver. Further, allometrically scaling rat nasal tissue enzyme activities has not been experimentally shown to be an appropriate, accurate method for approximating human values.

TABLE 3
Vmax values for the full activity, intermediate activity, and zero activity genotypes

	Vmax (nmol/min/ml)		
Tissue	High activity ALDH2*1/1	Intermediate activity ALDH2*1/2	No activity ALDH2*2/2
Dorsal respiratory epithelium	600	78	0
Ventral respiratory epithelium	600	78	0
Dorsal olfactory submucosa	600	78	0

The Distribution of Human ALDH2 Polymorphisms

Two key variants of the wild-type ALDH2 allele have been identified: ALDH2*1, an active form of the enzyme that is dominant in most populations studied, and ALDH2*2, an inactive form of the enzyme that is relatively common only in Asians. Three genotypes and their corresponding phenotypes are expected: a fully active homozygote (ALDH2*1/1, full activity), an intermediate activity heterozygote (ALDH2*1/2, intermediate activity), and a zero activity homozygote (ALDH2*2/2, zero activity). The presence of this polymorphism is well studied and has been characterized in hepatic but not nasal tissue. It was assumed that polymorphisms observed in human hepatic ALDH2, as described by Ginsberg (Ginsberg et al., 2002), are qualitatively and quantitatively predictive of those in the nasal tissues. Ginsberg reports the hepatic activity associated with each of the genotypes (Ginsberg et al., 2002), which are 0.54, 0.07, and 0.0 μmol/min/g liver for the fully active, intermediate activity, and zero activity genotypes, respectively. Assigning a relative activity of 100% to the fully active homozygote, the activity of the intermediate activity heterozygote was 13% of the fully active homozygote. The zero-activity homozygote was assigned a relative activity of zero for the ALDH2 Vmax. The corresponding activity for each of the three genotypes was determined by multiplying the value in the base simulation (600 nmol/min/ml tissue) by the relative activity of the three genotypes (100%, 13%, and 0%) reported by Ginsberg. The resulting Vmax values are reported in Table 3.

Sensitivity Analysis

Sensitivity analyses were conducted for anterior dorsal olfactory epithelial acetaldehyde concentrations and submucosa H^+ concentration at 1, 50, and 1000 ppm. The minute ventilation rate used in the rat model analysis was 210 ml/min. The minute ventilation rate used in the human model was 13,890 ml/min, which corresponds to the default ventilation rate of 20 m^3/day used in U.S. EPA risk assessments. All parameters were evaluated and only those showing sensitivity coefficients $\geq$0.1 are presented

Downloaded By: [Battelle for the USDOE] At: 15:18 3 March 2008

in the results section. To establish the sensitivity of extraction to the ALDH2 Vmax under the conditions this parameter was optimized, sensitivity analyses were also conducted for acetaldehyde extraction at 1 and 1000 ppm at a flow rate of 50 ml/min. The analyses were conducted using the subroutines in ACSLXtreme (Ver. 2.3.0.12) using the central differences method. Sensitivity coefficients were log-normalized and multiplied by their respective parameter value, resulting in a sensitivity coefficient that can be interpreted as the ratio of the standardized change in model response (output) to the standardized change in parameter values (input).

RESULTS

Calibration of Nasal Metabolism

Since nasal extraction is a function of the same processes that govern the nasal tissue concentration, a comparison of the model-derived extraction estimates to the measured nasal vapor uptake can provide a partial verification of the model-predicted tissue concentrations.

Morris and co-workers measured upper respiratory tract extraction (absorbed dose) in the surgically isolated upper respiratory tract of SD rats exposed unidirectionally to acetaldehyde at multiple flow rates (50–300 ml/min) and at multiple concentrations (10–1000 ppm) (Morris, 1999). Because extraction is a function of nasal tissue acetaldehyde metabolism, the Vmax for the high-affinity ALDH2 pathway was optimized to the upper-respiratory-tract extraction data. The resulting Vmax, 600 nmol/min/ml, described well the nonlinear behavior in extraction as a function of both the flow rate and concentration (Figure3). The model estimates for the nasal uptake correspond well to measured values over the 50–1000 ppm exposure range, except for underprediction at the lowest and mid concentration of the low flow rate and the lowest concentration at the mid (100 and 200 ml/min) flow rates. The model will be exercised for the rat portion of the interspecies dose extrapolation. Extraction was underpredicted at the lowest concentration in the 100 and 200 ml/min experiments. It is not clear why the model would be less accurate for these flow rates, but accurate for flows bracketing these (50 and 300 ml/min). New advances in modeling both airflow and metabolism in the tissue phase with a PBPK-directed computational fluid dynamics (CFD) structure (Schroeter et al., 2006) may improve model performance.

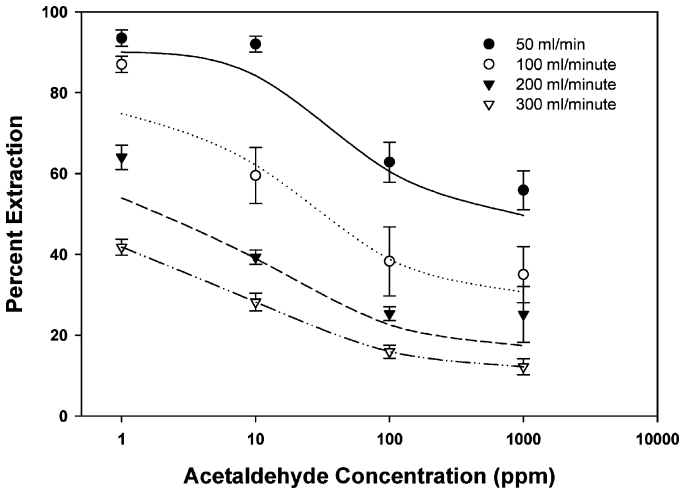

FIG. 3. Comparison of the observed (symbols) and model predicted extraction (lines) of acetaldehyde in the rat upper respiratory tract for a wide range of exposure concentrations and flow rates. Data are from Morris (1997). The rat ALDH2 Vmax was calibrated to these data.

The optimized rat ALDH2 Vmax of 600 nmol/min/ml tissue for respiratory and olfactory tissue compared well to values obtained by scale-up of the ALDH2 Vmax values reported by Casanova-Schmitz (Casanova-Schmitz et al., 1984). The scale-up was conducted by determining the composite factor that Bogdanffy (1998) used to scale up the ALDH1 activity reported by Casanova-Schmitz (Casanova-Schmitz et al., 1984), and then applying this value to the ALDH2 Vmax. The composite factor was calculated as the ratio of a) the ALDH1 Vmax Bogdanffy obtained by scale-up (mg/hr) to b) the ALDH1 Vmax reported by Casanova-Schmitz (1984) (nmoles/min/mg protein) and scaled up by Bogdanffy (1998). For respiratory epithelium, the value was 0.0264, and for olfactory submucosa, the value was 0.0336. The resulting values for the ALDH2 Vmax were 353 nmol/min/ml tissue for the respiratory epithelium and 659 nmoles/min/ml tissue for the olfactory submucosa, values sufficiently similar to the value of 600 nmol/min/ml tissue obtained by optimization.

Comparative Dosimetry

Acetaldehyde flux and acetaldehyde tissue concentrations are linearly related to the inhaled concentration of acetaldehyde in dorsal olfactory and ventral respiratory tissues of both rats and humans with fully functional ALDH (ALDH2*1/1). In both tissues, acetaldehyde flux is greater in humans than in rats, though both tissue acetaldehyde and H^+ were predicted to be lower in humans (Figures 4 and 5).

Tissue H^+ levels deviated somewhat from linearity with acetaldehyde exposure concentration, showing an initial rapid rise in concentration as exposure increased from 1–50 ppm acetaldehyde, after which the slope decreased somewhat (Figures 4 and 5).

Rat acetaldehyde flux and tissue concentrations as well as tissue H^+ are reported for the anterior dorsal olfactory and anterior ventral respiratory tissues at concentrations equal to those used in the chronic bioassay (Woutersen et al., 1986) in Table 4.

The Impact of Polymorphisms on Human Dosimetry

The results of simulations of nasal tissue dose metrics for the three high-affinity ALDH2 genotypes, i.e., high activity, intermediate activity, and no activity, are presented in Table 5. Reduced acetaldehyde clearance in heterozygote intermediate

Downloaded By: [Battelle for the USDOE] At: 15:18 3 March 2008

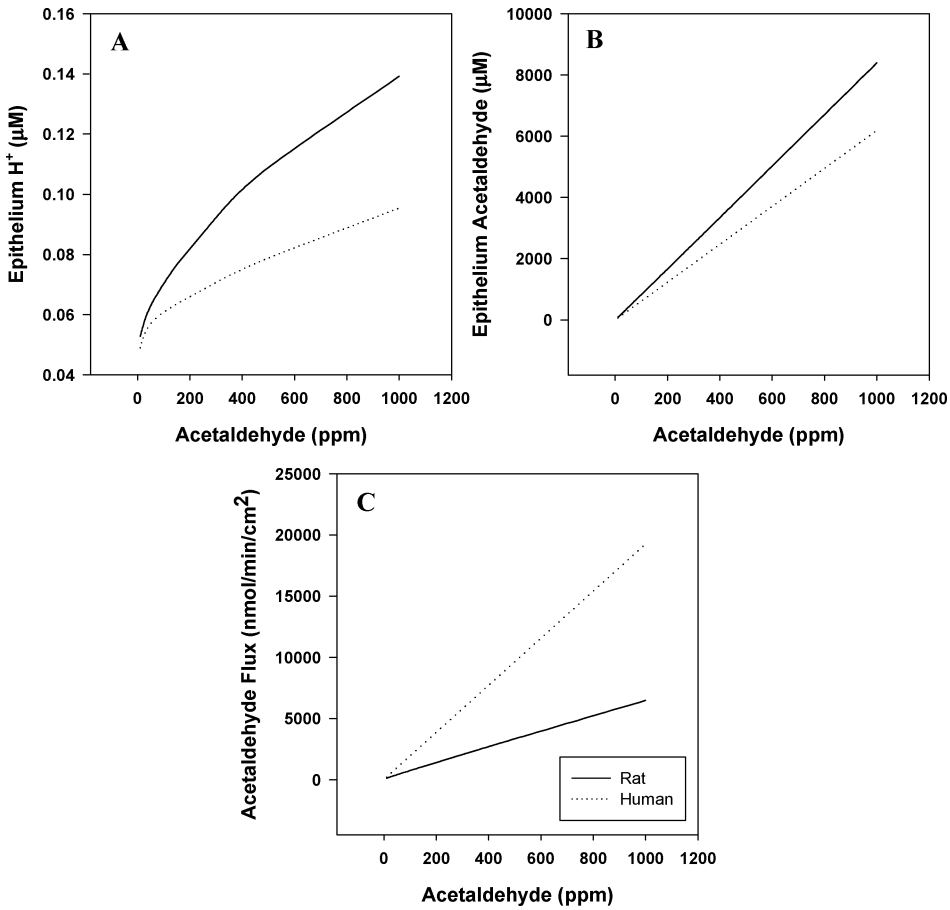

FIG. 4. Comparative rat and human dosimetry of steady-state submucosal H^+(A), epithelial tissue acetaldehyde concentration (B), and flux (C) in anterior dorsal olfactory tissue. Solid lines represent rat simulations; dotted lines represent human simulations.

activity individuals had a minimal effect on acetaldehyde concentrations and acetaldehyde flux in respiratory and olfactory epithelium and on pH or H^+ concentration in the respiratory epithelium and olfactory submucosa. The effect was greatest at low exposures, where tissue acetaldehyde concentrations were near the Km of 30 μM. For example, the acetaldehyde concentrations in dorsal olfactory epithelial tissue were only 6% higher for the zero activity genotype than for the full activity genotype at exposures of 10 ppm acetaldehyde, and 0.6% higher at exposures of 150 ppm acetaldehyde. The olfactory submucosa tissue pH was only 1% lower (more acidic) in the full activity compared with the zero activity group for exposures of 10 ppm acetaldehyde and 1.5% lower for exposures of 150 ppm acetaldehyde. This suggests a minimal role for ALDH2 in the metabolic clearance of acetaldehyde and metabolic acidification of nasal tissues following exposure to acetaldehyde and other compounds producing acetaldehyde in the course of normal metabolism, even at low exposures. The ALDH1 pathway is responsible for a preponderance of the total acetaldehyde metabolism, at least at these experimental doses and flow rates.

Distribution of Nasal Tissue Dose Metrics in the Human Population

The overall distribution of acetaldehyde metabolism related tissue dose metrics in the population will follow the frequency of the genotypes, which is a function of the ethnic make up of the population. The percent of individuals having each of the three ALDH2 genotypes within several ethnic groups (Ginsberg et al., 2002) are presented in Table 5. African and Mexican and Caucasian Americans have the highest frequency of the fully active ALDH2 allele while Asian ethnic groups have the lowest.

Human Equivalent Concentrations

Equations describing the acetaldehyde exposure: dose relationships for rats and humans were developed to replace the need to use the acetaldehyde PBPK model. The equations empirically relate exposure and tissue dose at steady state and do not account for exposure duration in the rodent studies, as Dorman et al. (2008) do for derivation of an inhalation reference concentration (RfC) for acetaldehyde. Equations for exposure: anterior

Downloaded By: [Battelle for the USDOE] At: 15:18 3 March 2008

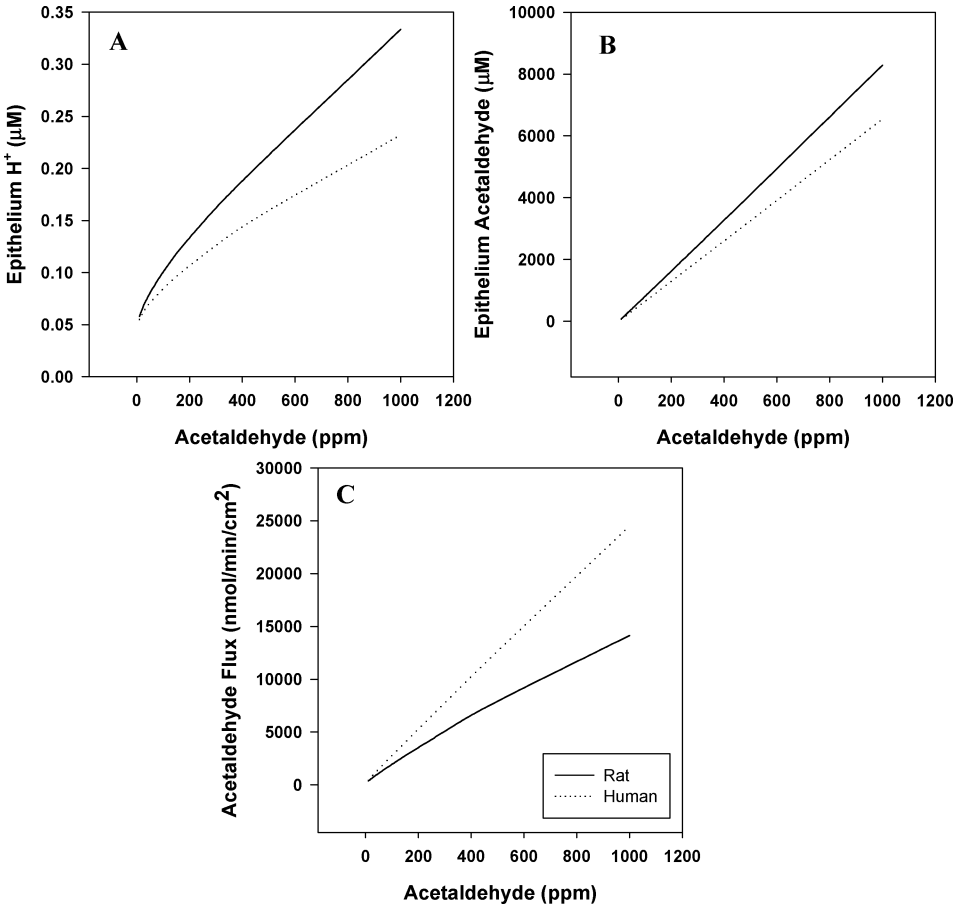

FIG. 5. Comparative rat and human dosimetry of steady-state submucosal H^+(A), epithelial tissue acetaldehyde concentration (B), and flux (C) in anterior ventral respiratory tissue. Solid lines represent rat simulations; dotted lines represent human simulations.

dorsal olfactory acetaldehyde flux [Eq. (1)], epithelial tissue concentration [Eq. (2)], and exposure:dorsal olfactory submucosa H^+ concentration [Eq. (3)] are provided below. R designates rat, H, human. The R-squared for all fits was $\geq$.99.

$$\text{Flux} = 6.41 \times \text{ppm} + 110 \quad [1^R]$$

$$\text{Flux} = 19.2 \times \text{ppm} + 28.21 \quad [1^H]$$

$$\text{Acetaldehyde Concentration } (\mu\text{M}) = 8.41 \times \text{ppm} - 14.7 \quad [2^R]$$

$$\text{Acetaldehyde Concentration } (\mu\text{M}) = 6.20 \times \text{ppm} - 7.5 \quad [2^H]$$

$$\text{Proton Concentration } (\mu\text{M}) = 1.4 \times 10^{-4} \times \text{ppm} - 5.7 \times 10^{-8} \times \text{ppm}^2 + 0.054 \quad [3^R]$$

$$\text{Proton Concentration } (\mu\text{M}) = 7.2 \times 10^{-5} \times \text{ppm} - 2.8 \times 10^{-8} \times \text{ppm}^2 + 0.051 \quad [3^H]$$

By combining rat and human equations, we can solve for the human equivalent concentration for each dose metric. Equations (4) and (5) can be used to directly calculate the human equivalent concentration (HEC) from a rat acetaldehyde concentration in ppm based on flux [Eq. (4)], or anterior dorsal olfactory epithelial acetaldehyde concentration [Eq. (5)]. The HEC based on anterior dorsal olfactory submucosal H^+ concentration is best calculated by separately solving Eq. (3) for the rat and human.

$$HEC_{\text{flux}} = (6.41 \times \text{ppm}^{\text{Rat}} + 81.8)/19.2 \quad [4]$$

$$HEC_{\text{Acetaldehye}(\mu\text{M})} = (8.41 \times \text{ppm}^{\text{Rat}} - 7.2)/6.2 \quad [5]$$

The human equivalent concentration to the rat NOAEL of 50 ppm based on steady-state acetaldehyde concentrations from continual exposures was 67 ppm. The impact of presumed ALDH2 polymorphisms the HEC calculation was negligible; the human equivalent acetaldehyde concentration for homozygous low activity was 66 ppm, 1.5% lower than for the homozygous full activity phenotype.

Derivation of an RfC requires two additional adjustments, one for exposure duration and one for uncertainty factors. These adjustments are applied by Dorman et al. (2008).

Sensitivity Analysis

Under the experimental conditions used to optimize the ALDH2 Vmax, acetaldehyde extraction was differentially sensitive to the ALDH1 and ALDH2 Vmax values. At 1 ppm acetaldehyde and a flow rate of 50 ml/min, the sensitivity coefficient

Downloaded By: [Battelle for the USDOE] At: 15:18 3 March 2008

TABLE 4
Rat dose metrics for concentrations of atmospheric acetaldehyde in the subchronic and chronic inhalation assays

	Anterior dorsal olfactory				Anterior ventral respiratory			
	Epithelial	Submucosa						
Exposure (ppm)	Acetaldehyde (μM)	pH	H^+ (μM)	Flux[a]	Acetaldehyde (μM)	pH	H^+ (μM)	Flux[a]
Subchronic inhalation bioassay								
50	409	7.2	0.06	420	395	7.1	0.08	1109
150	1244	7.1	0.077	1085	1212	7.0	0.118	2765
400	3340	7.0	0.101	2710	3272	6.7	0.188	6537
500	4181	7.0	0.109	3350	4102	6.7	0.213	7929
1000	8399	6.9	0.139	6487	8286	6.5	0.333	14,135
2200	18,582	6.7	0.183	13,749	18,475	6.1	0.816	25,951
5000	42,467	6.6	0.233	30,094	42,557	[b]	[b]	47,073
Chronic inhalation bioassay								
750	6287	6.9	0.13	4930	6188	6.6	0.27	11,171
735	6161	6.9	0.125	4836	6062	6.6	0.269	10,985
1412	11,888	6.8	0.157	9013	11,767	6.4	0.447	18,562
1500	12,634	6.8	0.16	9547	12,513	6.3	0.47	19,449
1527	12,863	6.8	0.162	9711	12,742	6.3	0.484	19,717

Note. Dose metrics are reported for the epithelial layer of the listed tissue, except for pH and H^+ concentration in the olfactory tissue, which are reported for the submucosa.

[a]Flux is defined as the nanomoles of acetaldehyde moving from the air phase into the corresponding epithelial tissue per minute and per square centimeter of tissue surface area. Units are nmol/min/cm^2.

[b]Proton production exceeds the buffering capacity of the cell or the capacity of the antiport, resulting in molar concentrations of protons, which are not physiologically realistic.

(SC) for the ALDH2 Vmax was 0.37, and the ALDH1 Vmax was zero, indicating that the low-concentration, low-flow-rate exposure extraction data set was appropriate for deriving the ALDH2 Vmax.

Dorsal olfactory epithelial tissue acetaldehyde concentrations in both the rat and human were sensitive to parameters influencing uptake—tissue air partition coefficient, minute ventilation rates and tissue thickness, and some influencing clearance—nasal blood flow and tissue blood partition coefficient (Tables 6 and 7). Tissue acetaldehyde concentrations were not sensitive to metabolic clearance (ALDH metabolic parameters).

Dorsal olfactory submucosa H^+ concentration was most sensitive to the Vmax and the Hill coefficient for the proton antiport, dorsal olfactory tissue thickness. High-affinity ALDH metabolic constants influenced H^+concentrations at high acetaldehyde exposure levels (Tables 6 and 7). H^+ concentrations showed greater sensitivity (0.25 vs. 0.1) to nasal tissue blood flow in rats than humans.

DISCUSSION

The current RfC for acetaldehyde in the U.S. Environmental Protection Agency (EPA) Integrated Risk Information System (IRIS) is based on an HEC derived using the default cross-species dosimetry approach for category 1 (reactive) gases (U.S. EPA, 1994). This categorical default approach calculates a regional gas dose ratio (RGDR) between the human and the experimental animal on the basis of ventilation rate and extrathoracic surface area, assuming a high mass transfer coefficient in each species. In the case of the acetaldehyde RfC, the default RGDR was calculated to be 0.18, resulting in an HEC that is a factor of 5.6 lower than the duration-adjusted NOAEL in the rat. However, more recent developments in the area of computational fluid dynamic (CFD) and PBPK modeling of the nose have made it possible to provide chemical-specific RGDRs for many category 1 gases (Frederick et al., 1998; Kimbell et al., 1997; Morris et al., 1993; Plowchalk et al., 1997). In some cases, chemical-specific analyses for category 1 gases have resulted in RGDRs closer to unity than the default approach (Andersen et al., 1999). The model described here can be used to provide chemical-specific dosimetry in support of future risk assessments for acetaldehyde based on its nasal toxicity in the rat.

With the exception of H^+ concentrations, which were somewhat nonlinear across the range of tested concentrations, acetaldehyde tissue concentrations and flux are linearly related to acetaldehyde exposure in both the dorsal olfactory and

Downloaded By: [Battelle for the USDOE] At: 15:18 3 March 2008

TABLE 5
Human nasal tissue dose metrics at various concentrations of atmospheric acetaldehyde for the three genotypes: full, intermediate, and zero activity

	Anterior dorsal olfactory[a]				Anterior ventral respiratory[a]			
Exposure (ppm)	AALD (μM)	pH	H^+ (μM)	Flux[b]	AALD (μM)	pH	H^+ (μM)	Flux[b]
Human full activity: Frequency distribution: African American (100%), Mexican American (100%), Caucasian (99%), Chinese (57%), Japanese (53%), Korean (71%)								
10	58	7.31	0.049	210	58	7.26	0.055	423
50	303	7.24	0.057	995	315	7.15	0.071	1505
150	921	7.20	0.064	2919	965	7.02	0.096	4038
300	1849	7.15	0.071	5801	1944	6.90	0.126	7768
500	3087	7.10	0.079	9644	3253	6.80	0.160	12,650
1000	6190	7.02	0.095	19,261	6541	6.63	0.232	24,490
Human intermediate activity: Frequency distribution: Caucasian (1%), Chinese (39%), Japanese (43%), Korean (27%)								
10	61	7.38	0.042	195	64	7.34	0.046	277
50	308	7.34	0.045	964	324	7.22	0.061	1301
150	926	7.29	0.052	2884	975	7.06	0.088	3821
300	1854	7.23	0.060	5764	1954	6.93	0.118	7547
500	3093	7.16	0.069	9607	3263	6.82	0.152	12,427
1000	6196	7.06	0.086	19,223	6551	6.65	0.224	24,265
Human zero activity: Frequency distribution: Chinese (5%), Japanese (5%), Korean (2.5%)								
10	62	7.39	0.041	192	65	7.35	0.044	255
50	309	7.36	0.043	959	325	7.23	0.059	1270
150	927	7.30	0.050	2879	976	7.06	0.086	3788
300	1855	7.24	0.058	5759	1955	6.93	0.117	7514
500	3094	7.17	0.067	9602	3264	6.82	0.151	12,394
1000	6197	7.07	0.085	19,218	6552	6.65	0.223	24,231

Note. The expected frequency (Ginsberg et al., 2002) of the listed dose metric for several ethnic groups is presented. Small errors in frequency associated with rounding values to two significant figures result in total percentages slightly more than 100%.

[a]Dose metrics are reported for the epithelial layer of the listed tissue, except for pH and H^+ concentration in the olfactory tissue, which are reported for the submucosa. The model was run at the given exposure to steady state, the period of exposure after which additional exposure has no impact on dose metrics.

[b]Units are nmol/min/cm^2.

ventral respiratory epithelium. The metabolic and biochemical processes controlling intracellular pH and acetaldehyde levels are energy dependent and saturable. Such systems are inherently nonlinear, but appear only to be so outside the range of acetaldehyde exposure concentrations important for interpreting the rat acetaldehyde toxicity and carcinogenicity data sets. One outcome of the linearity of the exposure:tissue dose relationships is that applying uncertainty factors at either the HEC or the rodent target tissue concentration prior to back extrapolation of the HEC, will yield the same RfC. This is not always the case. When the exposure-tissue dose relationship is nonlinear in either the test species or humans, applying the uncertainty factors at the level of the tissue dose will lead to a different RfC than if the uncertainty factors are applied to the HEC. However, a consensus has not been reached regarding which approach is most appropriate.

Acetaldehyde tissue concentrations and flux increased at a much higher rate in both the dorsal olfactory and ventral respiratory tissues compared with submucosal H^+concentrations. Changes in proton concentrations were on the order of three- to sixfold across a 100-fold increase in acetaldehyde exposure while acetaldehyde flux and tissue concentrations increased ~100-fold, in direct proportion to acetaldehyde exposure. This difference reflects the increased control the tissue exerts over H^+ concentrations. Since stoichiometrically, two protons are produced from each mole of acetaldehyde metabolized, the activity

Downloaded By: [Battelle for the USDOE] At: 15:18 3 March 2008

TABLE 6
Rat model sensitivity analysis

Parameter	Acetaldehyde concentration (ppm) 1 ppm	50 ppm	1000 ppm
Dorsal olfactory epithelium acetaldehyde concentration			
AALD metabolism—ALDH2			
Km	0.11	—	—
Minute ventilation	0.17	—	—
Partition coefficients			
Blood air	0.85	0.95	0.96
Tissue blood	1.04	1.02	1.02
Nasal blood flow	0.10	0.10	0.10
DO tissue thickness	0.50	0.50	0.50
Dorsal olfactory submucosa H^+ concentration			
AALD metabolism—ALDH1			
Vmax	—	0.11	0.49
Km	0.00	−0.10	−0.35
AALD metabolism—ALDH2			
Vmax	—	0.19	—
Partition coefficients			
Tissue/air	—	0.12	0.34
Nasal blood flow	0.10	0.10	0.10
DO tissue thickness	0.50	0.50	0.50
Proton antiport Vmax	—	−0.31	−0.57
Proton antiport Hill coefficient	0.15	0.68	0.5

TABLE 7
Human model sensitivity analysis

Parameter	Acetaldehyde concentration (ppm) 1 ppm	50 ppm	1000 ppm
Dorsal olfactory epithelium acetaldehyde concentration			
Minute ventilation	0.22	0.14	0.12
Partition coefficients			
Tissue/air	0.80	0.88	0.88
Tissue/blood	1.05	1.06	1.06
Nasal blood flow	0.25	0.25	0.25
DO tissue thickness	0.4	0.4	0.4
Dorsal olfactory submucosa H^+ concentration			
AALD metabolism—ALDH1			
Vmax	—	0.21	0.10
Partition coefficients			
Blood/air	—	—	0.27
Nasal blood flow	0.25	0.25	0.25
DO tissue thickness	0.4	0.4	0.4
Proton antiport Vmax	—	−0.27	−0.46
Proton antiport Hill coefficient	0.1	0.62	0.7

of the proton pumps must exceed the activity of ALDH for H^+ concentrations to change so little.

The available data describing of the hepatic Vmax for three variants of the human the high-affinity, low-capacity pathway for acetaldehyde metabolism (ALDH2) were used to explore the impact of corresponding, but unmeasured, reductions in nasal tissue ALDH2 activity would have on nasal tissue metabolism and tissue dosimetry. Measured ALDH2 activities show a limited capacity for acetaldehyde metabolism by ALDH2 in rat nasal tissues, which suggests a more limited role for ALDH2 and polymorphisms in ALDH2 to impact tissue acetaldehyde levels and risks from exposure to acetaldehyde. Human simulations, as expected, support this finding, demonstrating that polymorphisms in genes coding ALDH2 have very little impact on tissue aldehyde or H^+ concentrations. This should not be surprising; data in multiple rodent species (Morris, 1997) indicate that in nasal tissues, ALDH2 does not seem to be the major contributor to acetaldehyde metabolism as it may be in the liver. Regardless of the absolute impact on tissue doses, it is important to note that the presence of the ALDH2 polymorphism reducing acetaldehyde metabolism could increase or decrease risks associated with acetaldehyde exposure. If toxicity is solely driven by tissue acidification, the presence of the mutant ALDH2 allele describes a population with reduced risks (less acidification of the tissue), though the effect would be negligible. The opposite is true if toxicity is driven by tissue concentrations of acetaldehyde.

Understanding the dose-response relationships for acetaldehyde nasal tissue cytotoxicity and tumorigenicity is of importance to the risk assessment not only of acetaldehyde, but also of other acetaldehyde-producing compounds such as ethanol, ethyl acetate, and vinyl acetate. The U.S. EPA is currently conducting an IRIS review and risk assessment of acetaldehyde. In a process similar in some regards to the one taken by Dorman et al. (2008), the U.S. EPA IRIS review will produce dose-response relationships and risk assessment estimates for of acetaldehyde based on both its noncarcinogenic and carcinogenic effects. A question of considerable importance with regard to the impact of the U.S. EPA IRIS findings on the risk assessment of other chemicals is how the acetaldehyde findings can be extrapolated to other acetaldehyde producing chemicals so a consistent approach is taken to the contribution of acetaldehyde to the genotoxicity and cytotoxicity of these compounds. Vinyl acetate, for instance, is metabolized rapidly to acetaldehyde in rodent and human nasal tissues. Vinyl acetate is a rodent nasal carcinogen by the inhalation route. While it is plausible that the weak genotoxicity of acetaldehyde produced by metabolism of vinyl acetate drives nasal tumorigenesis, there is strong evidentiary basis supporting a mode of action (MOA) with intracellular acidification followed by cytotoxicity and subsequent compensatory

Downloaded By: [Battelle for the USDOE] At: 15:18 3 March 2008

cell proliferation as the key events in the mode of action for vinyl acetate (Bogdanffy et al., 1999b, 2001). Vinyl acetate inhalation studies result in coexposure to significant proton tissue concentrations and acetaldehyde. The role of acetaldehyde cannot be determined from such studies directly; rather, it must be inferred from mechanistic studies and by placing tissue acetaldehyde concentrations from vinyl acetate inhalation studies in the context of those from acetaldehyde inhalation studies. With the development of this acetaldehyde PBPK model, there exist nasal tissue dosimetry models for both acetaldehyde and vinyl acetate that can be used to compare acetaldehyde concentrations in nasal tissues at carcinogenic and noncarcinogenic/noncytotoxic acetaldehyde exposure concentrations to those from vinyl acetate exposures.

REFERENCES

Andersen, M. E., Sarangapani, R., Frederick, C. B., and Kimbell, J. S. 1999. Dosimetric adjustment factors for methylmethacrylate derived from a steady-state analysis of a physiologically based clearance-extraction model. *Inhal. Toxicol.* 11:899–923.

Appelman, L. M., Woutersen, R. A., and Feron, V. J. 1982. Inhalation toxicity of acetaldehyde in rats. I. Acute and subacute studies. *Toxicology* 23:293–307.

Appelman, L. M., Woutersen, R. A., Feron, V. J., Hooftman, R. N., and Notten, W. R. 1986. Effect of variable versus fixed exposure levels on the toxicity of acetaldehyde in rats. *J. Appl. Toxicol.* 6:331–336.

Bogdanffy, M. S., and Taylor, M. L. 1993. Kinetics of nasal carboxylesterase-mediated metabolism of vinyl acetate. *Drug Metab. Dispos.* 21:1107–1111.

Bogdanffy, M. S., Randall, H. W., and Morgan, K. T. 1986. Histochemical localization of aldehyde dehydrogenase in the respiratory tract of the Fischer-344 rat. *Toxicol. Appl. Pharmacol.* 82:560–567.

Bogdanffy, M. S., Sarangapani, R., Kimbell, J. S., Frame, R. S., and Plowchalk, D. R. 1998. Analysis of vinyl acetate metabolism in rat and human nasal tissues by an in vitro gas uptake technique. *Toxicol. Sci.* 46:235–246.

Bogdanffy, M., Sarangapani, R., Andersen, M., Jarabek, A., and Dellarco, V. 1999a. Inhalation hazard identification and dose-response characterization for vinyl acetate. DuPont Hasekll Laboratory, Newark, DE.

Bogdanffy, M. S., Sarangapani, R., Plowchalk, D. R., Jarabek, A., and Andersen, M. E. 1999b. A biologically-based risk assessment for vinyl acetate-induced cancer and non-cancer inhalation toxicity. *Toxicol. Sci.* 51:19–35.

Bogdanffy, M. S., Plowchalk, D. R., Sarangapani, R., Starr, T. B., and Andersen, M. E. 2001. Mode-of-action-based dosimeters for interspecies extrapolation of vinyl acetate inhalation risk. *Inhal. Toxicol.* 13:377–396.

Brown, R. P., Delp, M. D., Lindstedt, S. L., Rhomberg, L. R., and Beliles, R. P. 1997. Physiological parameter values for physiologically based pharmacokinetic models. *Toxicol. Ind. Health* 13:407–484.

Casanova-Schmitz, M., David, R., and Heck, H. 1984. Oxidation of formaldehyde and acetaldehyde by NAD^+-dependent dehydrogenases in rat nasal mucosal homogenates. *Biochem. Pharmacol.* 33:1137–1142.

Dellarco, V. L. 1988. A mutagenicity assessment of acetaldehyde. *Mutat. Res.* 195:L1–L20.

Dorman, D. C., Struve, M. F., Wong, B. A., Gross, E. A., Parkinson, C., Willson, G. A., Tan, Y.-M., Campbell, J. L., Teeguarden, J. G., Clewell, H. J. III, Andersen, M. E. Derivation of an inhalation reference concentration based upon olfactory neuronal loss in male rats following subchronic acetaldehyde inhalation. *Inhal. Toxicol.* 20:245–256.

Feron, V. J., Kruysse, A., and Woutersen, R. A. 1982. Respiratory tract tumours in hamsters exposed to acetaldehyde vapour alone or simultaneously to benzo(a)pyrene or diethylnitrosamine. *Eur. J. Cancer Clin. Oncol.* 18:13–31.

Feron, V. J., Til, H. P., de Vrijer, F., Woutersen, R. A., Cassee, F. R., and van Bladeren, P. J. 1991. Aldehydes: Occurrence, carcinogenic potential, mechanism of action and risk assessment. *Mutat. Res.* 259:363–385.

Franklin, J. L., and Johnson, E. M., Jr. 1994. Elevated intracellular calcium blocks programmed neuronal death. *Ann. NY Acad. Sci.* 747:195–204.

Frederick, C. B., Bush, M. L., Lomax, L. G., Black, K. A., Finch, L., Kimbell, J. S., Morgan, K. T., Subramaniam, R. P., Morris, J. B., and Ultman, J. S. 1998. Application of a hybrid computational fluid dynamics and physiologically based inhalation model for interspecies dosimetry extrapolation of acidic vapors in the upper airways. *Toxicol. Appl. Pharmacol.* 152:211–231.

Ginsberg, G., Smolenski, S., Hattis, D., and Sonawane, B. 2002. Population distribution of aldehyde dehydrogenase-2 genetic polymorphism: Implications for risk assessment. *Regul. Toxicol. Pharmacol.* 36:297–309.

Holmberg, K., Bake, B., and Pipkorn, U. 1989. Mucosal blood flow in the human nose following local challenge with histamine. *Allergy* 44:45–51.

Jakoby, W. B., Bend, J. R., and Caldwell, J. 1982. Aldehyde oxidizing enzymes. In *Metabolic basis of detoxication*, Vol. 1, pp. 261–275. New York: Academic Press.

Jones, A. W. 1995a. Measuring and reporting the concentration of acetaldehyde in human breath. *Alcohol Alcoholism* 30:271–285.

Jones, A. W. 1995b. Measuring and reporting the concentration of acetaldehyde in human breath. *Alcohol Alcoholism* 30:271–285.

Kimbell, J. S., Godo, M. N., Gross, E. A., Joyner, D. R., Richardson, R. B., and Morgan, K. T. 1997. Computer simulation of inspiratory airflow in all regions of the F344 rat nasal passages. *Toxicol. Appl. Pharmacol.* 145:388–398.

Knowles, S., Jarrett, I., Filsell, O., and Ballard, F. 1974. Production and utilization of acetate in mammals. *Biochem. J.* 142:401–411.

Morris, J. B. 1997. Uptake of acetaldehyde vapor and aldehyde dehydrogenase levels in the upper respiratory tracts of the mouse, rat, hamster and guinea pig. *Fundam. Appl. Toxicol.* 35:91–100.

Morris, J. B. 1999. A method for measuring upper respiratory tract vapor uptake and its applicability to quantitative inhalation risk assessment. *Inhal. Toxicol.* 11:943–965.

Morris, J. B., Hassett, D. N., and Blanchard, K. T. 1993. A physiologically based pharmacokinetic model for nasal uptake and metabolism of nonreactive vapors. *Toxicol. Appl. Pharmacol.* 123:120–129.

Oyama, T., Isse, T., Kagawa, N., Kinaga, T., Kim, Y. D., Morita, M., Sugio, K., Weiner, H., Yasumoto, K., and Kawamoto, T. 2005. Tissue-distribution of aldehyde dehydrogenase 2 and effects of the ALDH2 gene-disruption on the expression of enzymes involved in alcohol metabolism. *Front. Biosci.* 10:951–960.

Downloaded By: [Battelle for the USDOE] At: 15:18 3 March 2008

Paulsson, B., Bende, M., and Ohlin, P. 1985. Nasal mucosal blood flow at rest and during exercise. *Acta Otolaryngol*. 99:140–143.

Plowchalk, D. R., Andersen, M. E., and Bogdanffy, M. S. 1997. Physiologically based modeling of vinyl acetate uptake, metabolism, and intracellular pH changes in the rat nasal cavity. *Toxicol. Appl. Pharmacol*. 142:386–400.

Schroeter, J. D., Kimbell, J. S., Bonner, A. M., Roberts, K. C., Andersen, M. E., and Dorman, D. C. 2006. Incorporation of tissue reaction kinetics in a computational fluid dynamics model for nasal extraction of inhaled hydrogen sulfide in rats. *Toxicol. Sci*. 90:198–207.

Stewart, M. J., Malek, K., and Crabb, D. W. 1996. Distribution of messenger RNAs for aldehyde dehydrogenase 1, aldehyde dehydrogenase 2, and aldehyde dehydrogenase 5 in human tissues. *J. Invest. Med*. 44:42–46.

Stott, W. T., Ramsey, J. C., and McKenna, M. J. 1986. Absorption of chemical vapors by the upper respiratory tract of rats. In *Toxicology of the nasal passages*, ed. C. S. Burrows, pp. 191–210. Washington, DC: Hemisphere.

Subramaniam, R., Richardson, R., B., Morgan, K. T., Kepler, G., Kimbell, J. S., and Guilmette, R. A. 1998. Computational fluid dynamics simulations of inspiratory airflow in the human nose and nasopharynx. *Inhal. Toxicol*. 10:91–120.

U.S. Environmental Protection Agency. 1994. *Methods for derivation of inhalation reference concentrations and application of inhalation dosimetry.* Washington, DC: Office of Health and Environmental Assessment.

Woutersen, R., Appelman, L., Feron, V., and Van der Heijden, C. 1984. Inhalation toxicity of acetaldehyde in rats. II. Carcinogenicity study: Interim results after 15 months. *Toxicology* 31:123–133.

Woutersen, R. A., Appelman, L. M., Van Garderen-Hoetmer, A., and Feron, V. J. 1986. Inhalation toxicity of acetaldehyde in rats. III. Carcinogenicity study. *Toxicology* 41:213–231.

Woutersen, R. A., and Feron, V. J. 1987. Inhalation toxicity of acetaldehyde in rats. IV. Progression and regression of nasal lesions after discontinuation of exposure. *Toxicology* 47:295–305.

Yoon, M., Madden, M. C., and Barton, H. A. 2006. Developmental expression of aldehyde dehydrogenase in rat: A comparison of liver and lung development. *Toxicol. Sci*. 89:386–398.

Yoshida, A. 1992. Molecular genetics of human aldehyde dehydrogenase. *Pharmacogenetics* 2:139–147.

APPENDIX A

TABLE A1
The set of mass balance equations for uptake and distribution of acetaldehyde in the lumen, epithelium, and submucosa of the inhalation PBPK model

Mass balance in the airway lumen compartment:

$$V_l \frac{dC_l}{dt} = Q_a(C_{in} - C_l) - K_{lt}(C_l - C_t/H_{ta})$$

Mass balance in the epithelial layer:

$$V_t \frac{dC_t}{dt} = K_{lt}(C_l - C_t/H_{ta}) - K_{tx}(C_t/H_{tt} - C_x/H_{tb})$$

Mass balance in the submucosal layer:

$$V_t \frac{dC_t}{dt} = K_{tx}(C_t/H_{tt} - C_x/H_{tb}) - Q_b(C_x/H_{tb} - C_{ab}) - \frac{V_m C_x/H_{tb}}{K_m + C_x/H_{tb}}$$

where:

C_l, C_t, C_x—Chemical species concentration in lumen, tissue, and submucosa, respectively.
V_l, V_t, V_x—lumen, tissue, and submucosa compartment volumes, respectively.
Q_a,Q_b—air flow and blood flow rates, respectively.
K_{lt}, K_{tx}—lumen to tissue and tissue to blood mass transfer coefficient, respectively.
H_{ta}, H_{tt}, H_{tb}—tissue:air and tissue:tissue, and tissue:blood partition coefficient, respectively.
V_{max}, K_m—kinetic parameters for metabolism of acetaldehyde or acetic acid.

Downloaded By: [Battelle for the USDOE] At: 15:18 3 March 2008

APPENDIX B

TABLE B1
Calculation of tissue-specific Vmax values for the low-affinity ALDH1 pathway

	Vmax[a] (mg/h)		Tissue thickness in the model (cm)		Tissue surface area (cm^2) in the model		Tissue volume (cm^3) in the model		Vmax[b] (nmol/min/ml)	
Tissue	Rat	Human	Rat	Human	Rat	Human	Rat	Human	Rat	Human
Respiratory	4.58	88.2	0.005	0.005	6.5	124.5	0.0325	0.6225	53,307	53,596
Olfactory	1.48	2.31	0.005	0.004	6.75	13.2	0.03375	0.0528	16,588	16,549

[a]Bogdanffy et al. (1998).

[b]Vmax is calculated by dividing the whole nose activity for a given tissue type (e.g. respiratory epithelium) by the modeled tissue volume (Table 2) and correcting for molar and time units.